Supporting Information

Photoaging alters the aggregation behavior of functionalized-nanoplastics differently：Effects of leached organic matter and surface properties changing

Tingting Hu [1], Yandi Hu[2], Zhixiong Li [1*], Shuhan Yu [1], Juanjuan Liu [3], Jiawei Chen [1*]

[1] School of Earth Sciences and Resources, China University of Geosciences, Beijing 100083, P. R. China

[2] College of Environmental Sciences and Engineering, and State Environmental Protection Key Laboratory of All Material Fluxes in River Ecosystems Peking University, Beijing 100871, China

[3] Key Laboratory of Eco-Geochemistry, Ministry of Natural Resources of China, National Research Center for Geoanalysis, Beijing 100037, China

[*]Corresponding Author

Email: lizhixiong@cugb.edu.cn; chenjiawei@cugb.edu.cn

Phone: 86-10-82321959

Submission: December 20, 2025

Section S1. Fluorescence measurements and parallel factor analysis modeling

The three-dimensional fluorescence spectra of PDOM derived from pristine and photoaged NPs with different functional groups were obtained by the fluorescence spectrophotometer, with a total of 18 samples (including three parallel replicates per group). Scans were performed over an excitation (Ex) wavelength for emission scans was incrementally increased from 200 and 550 nm at a step size of 5 nm, while the emission (Em) wavelength range of 220 to 600 nm with a step size of 2 nm. Both excitation and emission slits were set to 10 nm. All samples were diluted to a consistent concentration (~6 mg C/L) to eliminate inner filter effect. The fluorescence responses to the DIW water were subtracted from the measured sample spectra to obtain the final EEM data of the samples. The fluorescence intensities were normalized to Raman units (R.U.) using the fluorescence intensity of the integrated Raman peak at 350 nm (Em). The EEMs of all PDOM samples were modeled using the DOMfluor toolbox in Matlab R2024a, and the number of independent fluorescent components was determined by parallel factor analysis (PARAFAC) through split-half analysis. The maximum fluorescence intensity (F_{max}) of the peak of the identified components was used to represent the relative quantities of the individual DOM components.

Section S2. Adsorption experiment

First, the pristine and photoaged PSNPs were subjected to three to five washes with deionized water until the filtrate exhibited negligible UV absorbance (<0.002 Abs

at 254 nm), confirming complete elution of PDOM. Since the concentration of PSNPs varied during the washing process, the concentrations of washed pristine and photoaged PSNPs were quantified using UV-Vis spectrophotometry for subsequent adsorption experiments. The method referred to previous studies.[1]

Single point adsorption experiments were conducted to obtain the adsorbed mass (q, mg/g) of PDOM on various NPs. Prior to mixing, the pH values of both PSNPs suspensions and PDOM stock solutions was adjusted to 6.0 ± 0.3 using 10 mM NaOH and HCl. In each 40 ml glass vial, PSNP suspension was added into the PDOM solutions, where the final concentrations of PSNPs and PDOM were 10 mg/L and 2.0 mg C/L, respectively. The vials were shaken at 150 rpm and equilibrated for 48 h. Subsequently, the mixture was transferred to centrifugal filters with a molecular weight cutoff (MWCO) of 100 kDa and centrifuged at 5000 g for 2 min. The organic carbon content in the filtrate was then measured using a total organic carbon analyzer.

The adsorbed mass (q) of PSNPs was calculated using the eq (S1).

$$q = \frac{(C_0 - C_i) \times V}{m} \quad \text{(S1)}$$

Where, C_0 (mg C/L) and C_i (mg C/L) are the initial and final PDOM concentrations, respectively. V (L) is the volume of solution and m (g) is the mass of the PSNPs.

Section S3. Derjaguin- Landau-Verwey-Overbeek (DLVO) theory and the XDLVO calculations

The total interaction energy of different PSNPs was calculated with Derjaguin-Landau-Verwey-Overbeek (DLVO) theory and the extended DLVO (XDLVO) theory considering the Lewis acid-base interaction or repulsive steric interaction.

In DLVO theory, the total interaction energy is the sum of van der Waals interaction (V_{VDW}) and the electrostatic double layer interaction (V_{EDL}) eq (S2):[2,3]

$$V_{TOT} = V_{VDW} + V_{EDL} \tag{S2}$$

The V_{VDW} can be calculated by eq (S3-S4):[2,4,5]

$$V_{VDW} = -\frac{A}{6}\left[\frac{2r^2}{h(4r+h)} + \frac{2r^2}{(2r+h)^2} + \ln\frac{h(4r+h)}{(2r+h)^2}\right] \tag{S3}$$

$$A = 24\pi h_0^2(\sqrt{\gamma_P^{LW}} - \sqrt{\gamma_w^{LW}})^2 \tag{S4}$$

where A is the Hamaker constant of PSNPs, r is the initial hydrodynamic radius of PSNPs, h is the separation distance between particles, h_0 represents the minimum equilibrium distance between particles and is assumed to be 0.157 nm,[6] and γ_P^{LW} and γ_w^{LW} are the Lifshitz-van der Waals interfacial tension parameters for PSNPs and water, respectively.

The V_{EDL} can be obtained eq (S5-S6):[3]

$$V_{EDL} = 64\pi\varepsilon_0\varepsilon_r\frac{r}{2}\left(\frac{K_BT}{e}\right)^2\left(\tanh\left(\frac{ze\varphi_p}{4K_BT}\right)\right)^2 exp(-kh) \tag{S5}$$

Where ε_0 is the permittivity of free space (8.854×10^{-12} C/V/m), ε_w is the dielectric

constant of water (78.5), k is the Boltzmann constant (1.38×10^{-23} J/K), φ_p is the ζ potential of PSNPs. κ is the Debye reciprocal length, and can be given as eq (S6):

$$\kappa = \sqrt{\frac{N_A e^2 \sum C_i Z_i^2}{\varepsilon_0 \varepsilon_w kT}} \quad \text{(S6)}$$

Where N_A is the Avogadro number (6.02×10^{23} mol^{-1}), Z is the valence of ions, e is the electron charge (1.60×10^{-19} C), C_i is the molar concentration of ions in the solution, T is temperature (298 K).

In the extended DLVO theory considering Lewis acid-base interaction, the total interaction energy (V_{TOT}) is expressed as eq (S7):[7]

$$V_{tot} = V_{VDW} + V_{EDL} + V_{AB} \quad \text{(S7)}$$

Where V_{AB} is the Lewis acid-base interaction energy, which can be calculated by eq (S8):[5,7,8]

$$V_{AB} = \pi r \lambda_w \Delta G_{h_0}^{AB} exp(\frac{h_0 - h}{\lambda_w}) \quad \text{(S8)}$$

Where λ_w is the water decay length for acid-base interactions (1 nm),[5] and $\Delta G_{h_0}^{AB}$ is the free energy adhesion at h_0, which is given as eq (S9):[6]

$$\Delta G_{h_0}^{AB} = -4(\sqrt{\gamma_p^+ \gamma_p^-} + \sqrt{\gamma_w^+ \gamma_w^-} - \sqrt{\gamma_p^+ \gamma_w^-} - \sqrt{\gamma_w^+ \gamma_p^-}) \quad \text{(S9)}$$

Where the subscript p represents PSNPs, w represents water, subscript "+" and "-" denote the electron-acceptor and electron-donor parameters of surface, respectively.

The values of γ_w^{Tot}, γ_p^+ and γ_p^- for PSNPs can be calculated from measuring the air-liquid-PSNPs contact angles (θ) using three different polarity probe liquids (water, glycerol, and diiodomethane) with known surface tension parameters and by solving Young-Dupré equation eq (S10):[6]

$$\gamma_i^{Tot}(1+cos\theta) = 2(\sqrt{\gamma_i^{LW}\gamma_p^{LW}} + \sqrt{\gamma_i^+\gamma_p^-} + \sqrt{\gamma_p^+\gamma_i^-}) \quad \text{(S10)}$$

where the subscript i represents water, glycerol, and diiodomethane, respectively. The surface tension parameters of three probe liquids were shown in Table S4.

With the leaching of PDOM, the total interaction energy (V_{TOT}) considering steric repulsion can be calculated by XDLVO theory, shown as eq (S11): [9,10]

$$V_{tot} = V_{VDW} + V_{EDL} + V_{STE} \quad \text{(S11)}$$

Assuming the adsorbed layer was uniform, the steric force (V_{STE}) can be calculated by eq (S12-S14). These equations determined the entropy loss and osmotic pressure upon overlap or mixing of the adsorbed layers (Vs,mix) and the elastic repulsion when the layers are compressed between the NPs (Vs,el).

$$V_{s,mix} = \frac{4\pi r k_B T}{v_1}\left(\Phi_2^a\right)^2\left(\frac{1}{2}-\chi\right)\left(\delta-\frac{h}{2}\right)^2 \quad ; \delta < h < 2\delta \quad \text{(S12)}$$

$$V_{s,mix} = \frac{4\pi r \delta^2 k_B T}{v_1}\left(\Phi_2^a\right)^2\left(\frac{1}{2}-\chi\right)\left(\frac{h}{2\delta}-\frac{1}{4}-\ln\frac{h}{\delta}\right); \quad \delta < h < 2\delta \quad \text{(S13)}$$

$$V_{s,el} = \frac{2\pi r k_B T \rho \delta^2 \bar{\Phi}_2^a}{M_2^a}\left\{\frac{h}{\delta}\ln\left[\frac{h}{\delta}\left(\frac{3-h/\delta}{2}\right)^2\right] - 6\ln\left(\frac{3-h/\delta}{2}\right) + 3\left(1-\frac{h}{\delta}\right)\right\}; 0 < h < \delta \quad \text{(S14)}$$

where v_1 is the molar volume of the solvent (2.99×10^{-29} m^3/ water molecule); χ is the Flory-Huggins solvency parameter (0.4); δ (nm) is the thickness of adsorbed PDOM, which is determined by subtracting the hydrodynamic radius of PSNPs before and after adsorption. According to DLS measurements, the δ for PS- Bare, PS-COOH, PS-NH_2, APS- Bare, APS-COOH, and APS-NH_2 was 2.9 0.5, 4.3, 5.4 2.0 and 3.9, respectively; ρ is the dry density of PDOM, which is 1.5 g/cm^3; M_2^a is the molecular weight of PDOM (3066 Da), which is derived from the previous study;[11] $\bar{\Phi}_2^a$ represents the effective volume fraction of the adsorbed PDOM layer and can be expressed as follows:

$$\bar{\Phi}_2^a = \frac{4Q}{3\rho\pi\left[(\delta + r)^3 - r^3\right]} \quad \text{(S15)}$$

where Q (kg/particle) is the adsorbed mass. It can be obtained from the adsorption experiment.

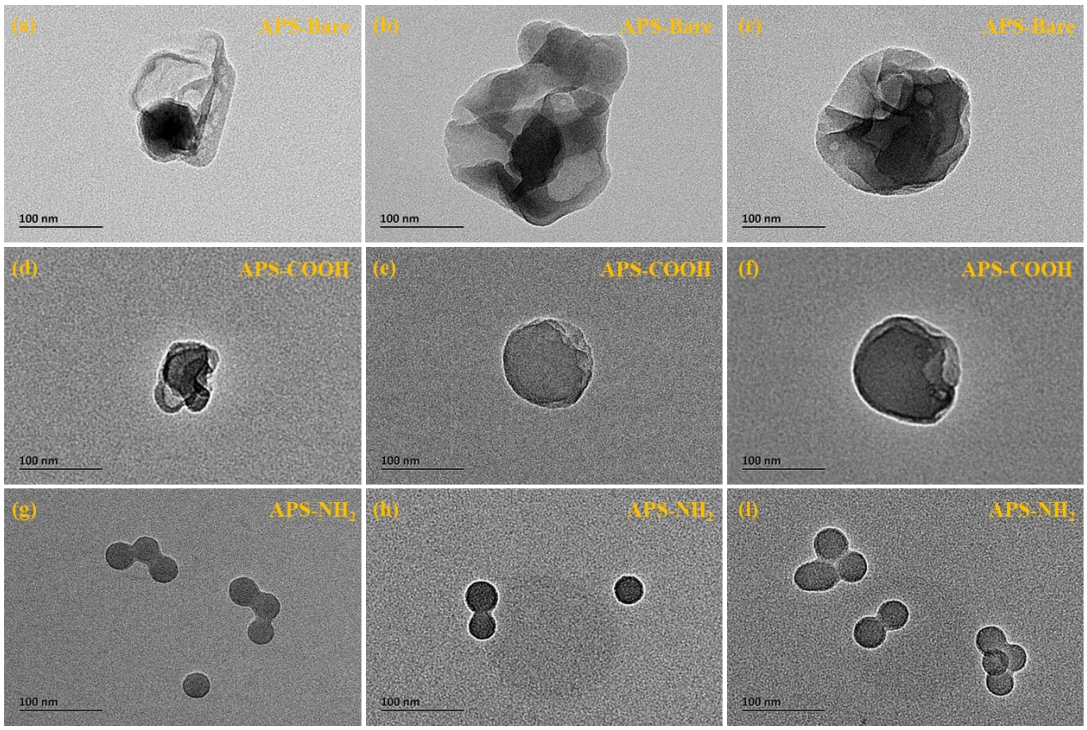

Fig. S1 TEM image of (a-c) APS-Bare, (e-g) APS-COOH, and (h-i) APS-NH_2 in deionized water.

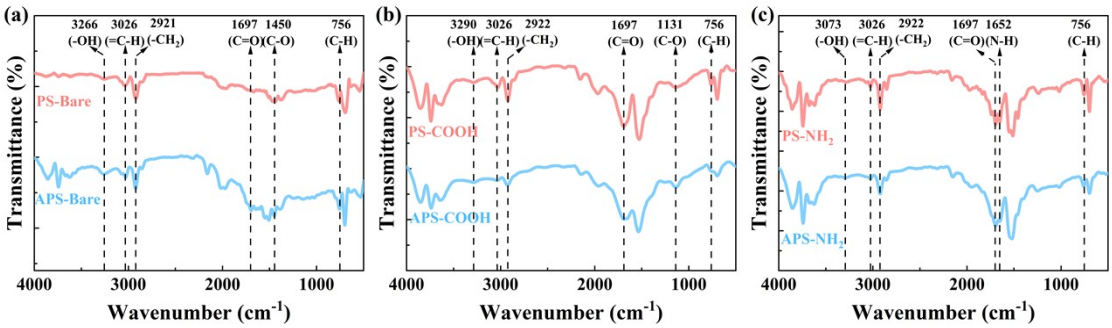

Fig. S2 ATR-FTIR spectrum for pristine and photoaged PSNPs: (a) PS-Bare, (b) PS-COOH, and (c) PS-NH_2.

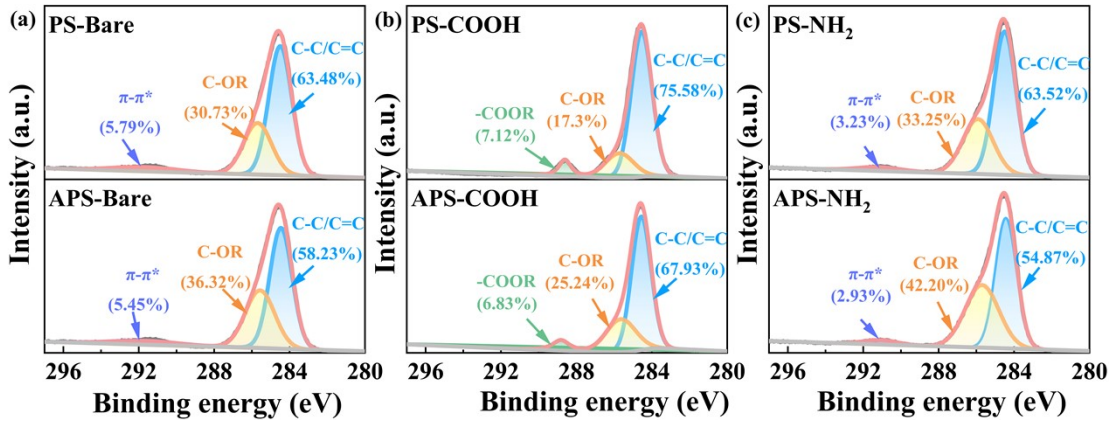

Fig. S3 High-resolution C1s XPS spectra of pristine and photoaged PSNPs: (a) PS-Bare, (b) PS-COOH, (c) PS-NH_2.

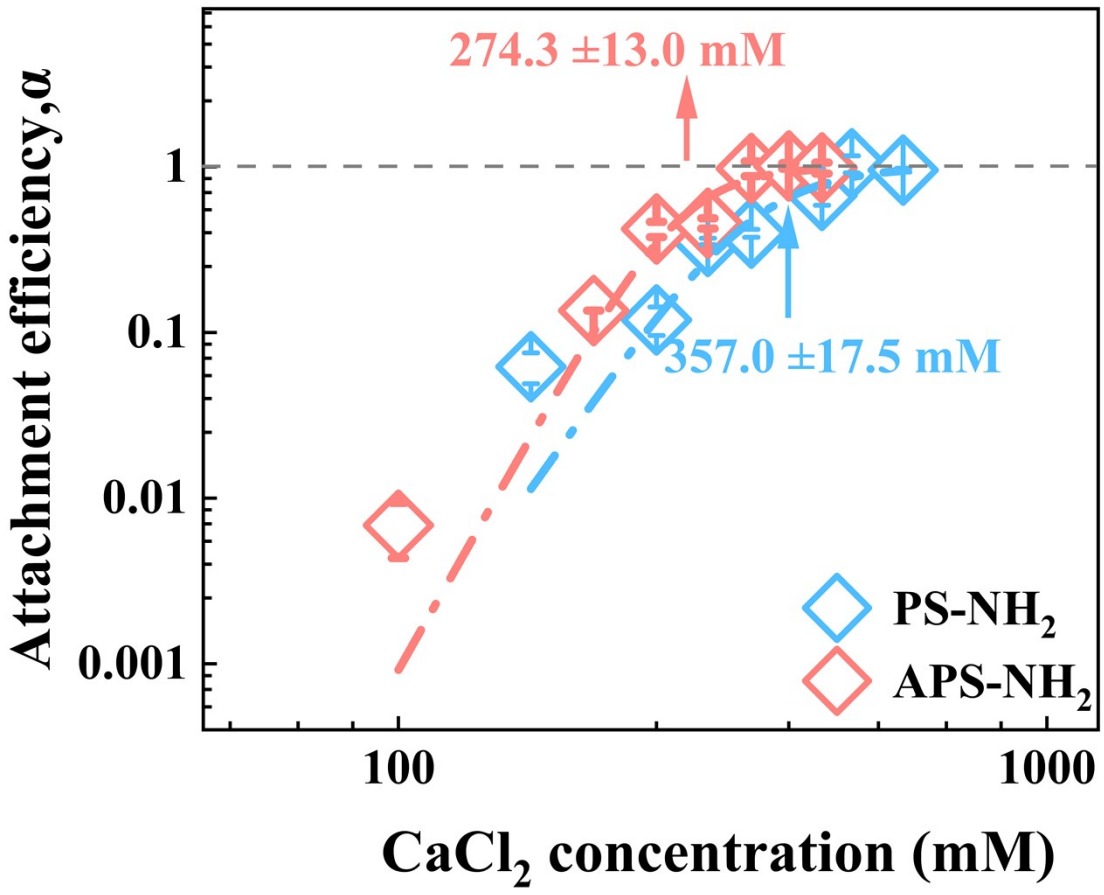

Fig.S4 Attachment efficiencies of pristine and photoaged PS-NH_2 in $CaCl_2$ solution at pH 6.

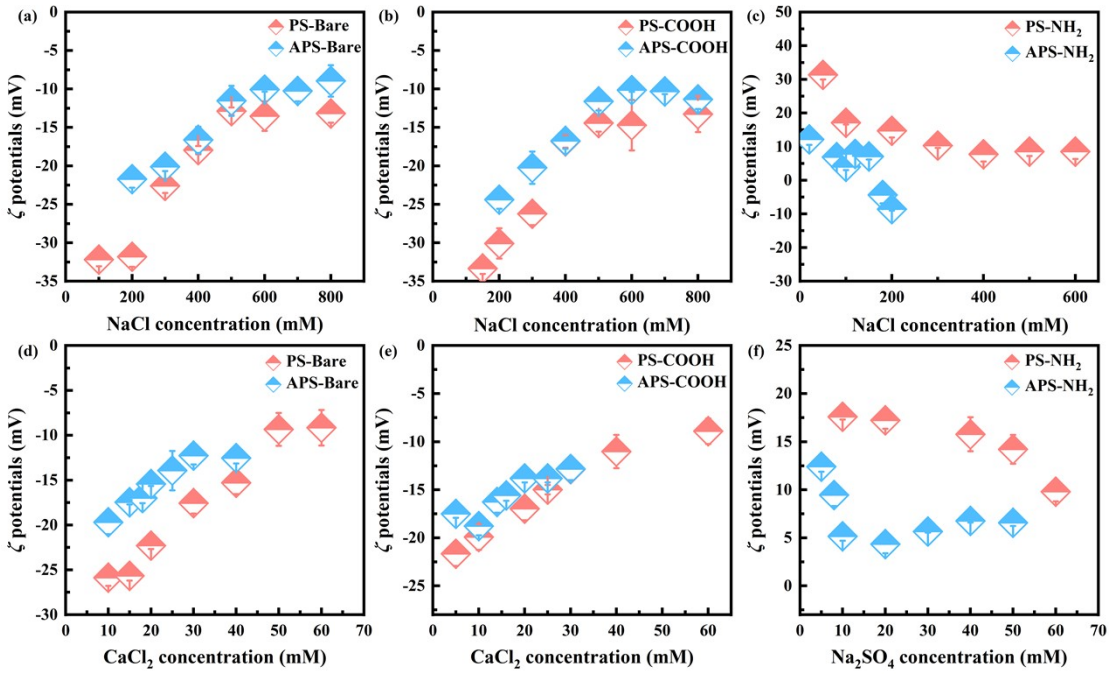

Fig. S5 Influence of photoaging on the ζ potentials of different functionalized PSNPs in (a-c) monovalent and (d-f) bivalent electrolyte solutions at pH 6: (a, d) PS-Bare and (b, e) PS-COOH in NaCl and $CaCl_2$ solution before and after photoaging, and PS-NH_2 in (c) NaCl and (f) Na_2SO_4 solution before and after photoaging.

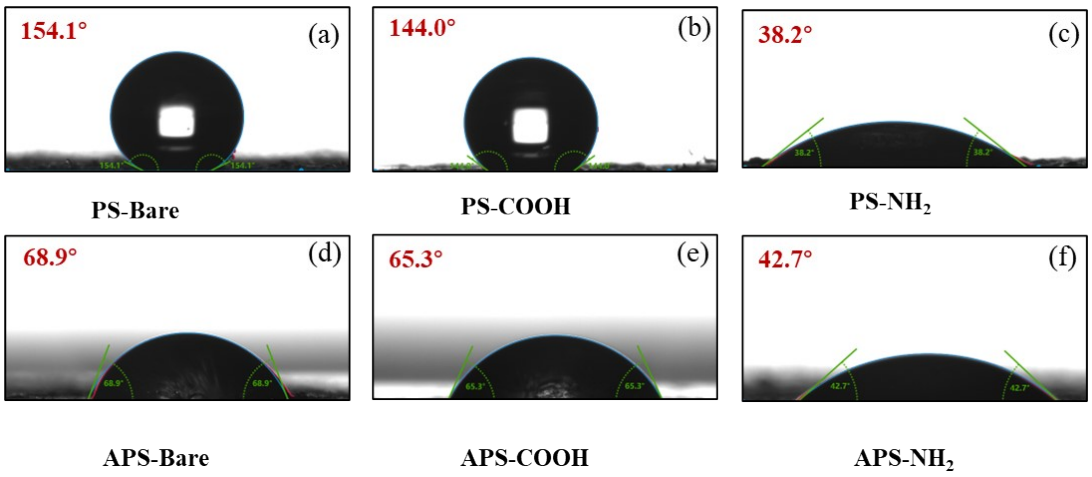

Fig. S6 Water contact angle of different functionalized PSNPs before and after photoaging：(a) PS-Bare, (b) PS-COOH, (c) PS-NH_2, (d) APS-Bare, (e) APS-COOH, (f) APS-NH_2.

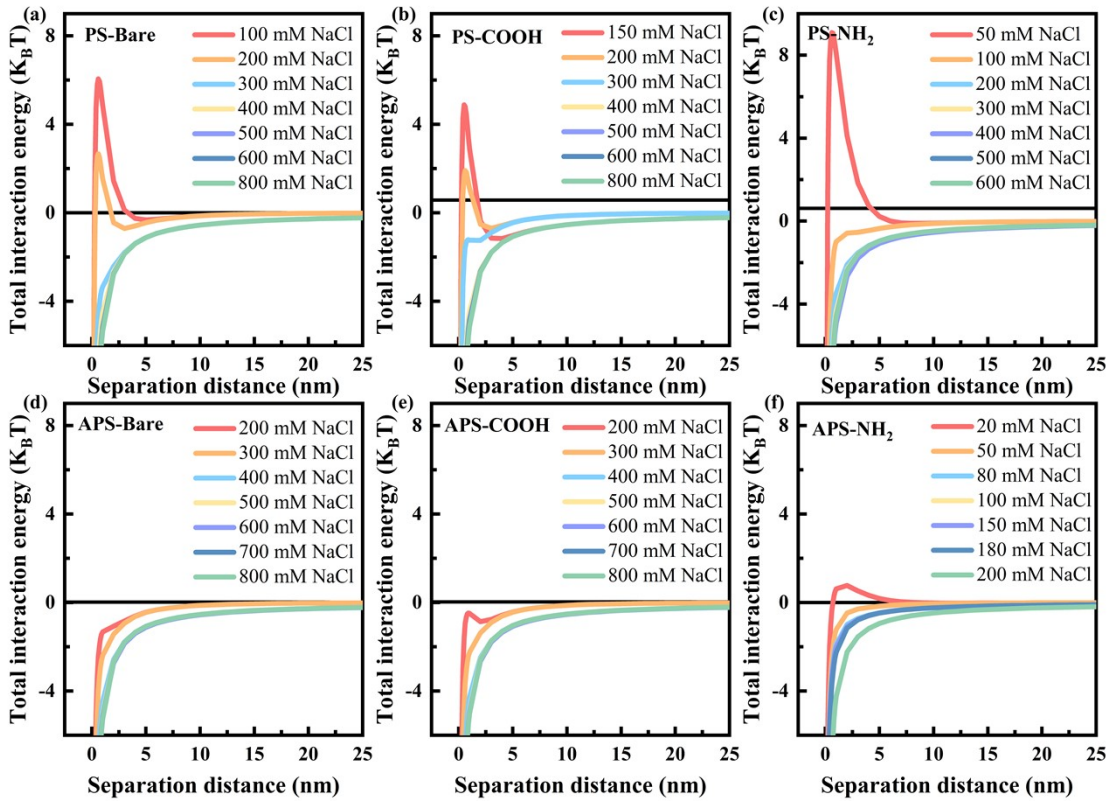

Fig. S7 Total interaction energy (G_{TOTAL}) profiles calculated with the classical DLVO theory for different functionalized PSNPs before and after photoaging in various NaCl solutions: (a) PS-Bare, (b) PS-COOH, (c) PS-NH_2, (d) APS-Bare, (e) APS-COOH, (f) APS-NH_2.

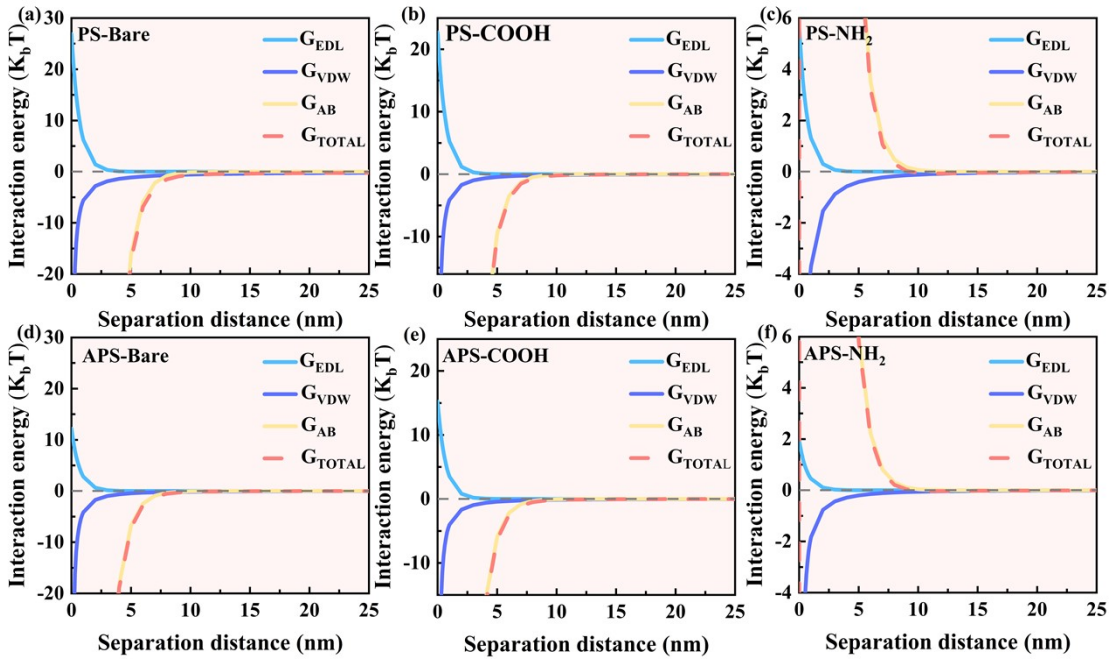

Fig. S8 The interaction energy of electrostatic force (G_{EDL}), Van der Waals force (G_{VDW}), Lewis acid-base interactions (G_{AB}), and the total interaction energy (G_{TOTAL}) for different functionalized PSNPs before and after photoaging in 200 mM NaCl solution: (a) PS-Bare, (b) PS-COOH, (c) PS-NH_2, (d) APS-Bare, (e) APS-COOH, (f) APS-NH_2.

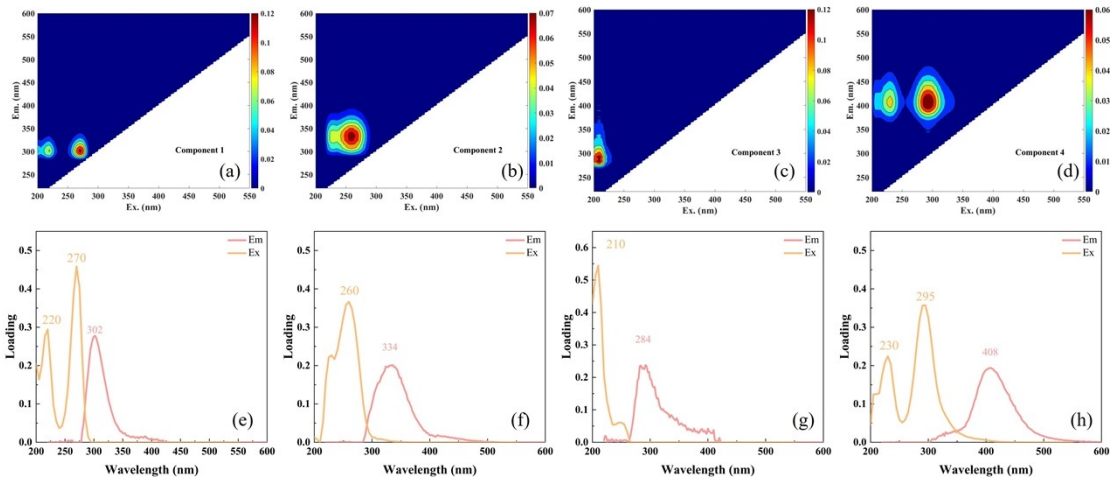

Fig. S9 The spectral characteristics (a-d) of four fluorescent components and the corresponding excitation/emission loadings (e-h) extracted from the EEM data sets of PDOM leached from pristine and photoaged PSNPs using PARAFAC modeling.

Table S1. Experimental conditions for aggregation kinetics of pristine and photoaged PSNPs

PSNPs type	electrolyte		pH
	Type	Concentration (mM)	
PS-Bare	NaCl	200, 300, 350 400, 450, 500, 600, 700, 800	6.0±0.3
	$CaCl_2$	10, 15, 20, 25, 30, 35, 40, 50, 60	
APS-Bare	NaCl	300, 400, 500, 550, 600, 700, 800, 900, 1000	
	$CaCl_2$	8, 10, 12, 15, 18, 20, 25, 30, 40	
PS-COOH	NaCl	150, 200, 300, 350, 400, 500, 600, 700, 800	
	$CaCl_2$	5, 10, 15, 20, 25, 30, 40, 60, 80	
APS-COOH	NaCl	350, 400, 500, 600, 650, 700, 800, 900, 1000	
	$CaCl_2$	8, 10, 12, 14, 16, 18, 20, 25, 30	
$PS-NH_2$	NaCl	50, 100, 200, 300, 350, 400, 500	
	$CaCl_2$	160, 250, 300, 350, 450, 500, 600	
	Na_2SO_4	10, 20, 30, 40, 50, 60, 70, 80	
$APS-NH_2$	NaCl	20, 50, 80, 100, 120, 150, 180, 200, 250	
	$CaCl_2$	100, 200, 250, 300, 350, 400, 450	
	Na_2SO_4	5, 7, 8, 10, 15, 20, 30, 40, 50	

Table S2. The surface tension parameter and adhesion free energy for different PSNPs calculated based on the contact angles of probe liquids.

Sample	Contact angle (degrees)			Surface tension (mJ m^{-2})			$\Delta G_{h_0}^{AB}$ (mJ m^{-2})	Hamaker constant (10^{-21} J)
	θ_W	θ_G	θ_D	γ^{LW}	γ^+	γ^-		
PS-Bare	154.1	61.2	6.6	50.46	9.85	80.69	-107.27	11.02
APS-Bare	68.9	48.8	11.2	49.83	0.94	5.32	-44.78	10.62
PS-COOH	144.0	49.0	11.2	49.84	15.49	82.57	-62.97	10.62
APS-COOH	65.3	42.7	14.1	49.28	1.65	5.97	-39.24	10.27
PS-NH_2	38.2	62.4	19.4	47.96	1.29	57.87	63.29	9.46
APS-NH_2	42.7	58.9	40.9	39.15	0.05	48.24	40.00	4.69

W, G, and D subscripts represent water, glycerol, and diiodomethane, respectively.

Table S3 The surface tension of the three probe liquids (mJ/m^2) [12]

Liquid	γ_w^{Tot}	γ_w^{LW}	γ_w^+	γ_w^-
Water	72.8	21.8	25.5	25.5
Glycerol	25.5	34.0	3.92	57.4
Diiodomethane	50.8	50.8	≈0	≈0

References

1 Y. Xu, X. Wang, J. P. van der Hoek, G. Liu and K. M. Lompe, Natural organic matter stabilizes pristine nanoplastics but destabilizes photochemical weathered nanoplastics in monovalent electrolyte solutions, *Environ. Sci. Technol.*, 2025, **59**, 1822-1834.

2 J. Gregory, Approximate expressions for retarded van der waals interaction, *J. Colloid. Interf. Sci.,* 1981, **83**, 138-145.

3 R. Hogg, T. W. Healy and D. W. Fuerstenau, Mutual coagulation of colloidal dispersions, *Trans. Faraday Soc.*, 1966, **62**, 1638.

4 F. Xu, C. Wei, Q. Zeng, X. Li, P. J. J. Alvarez, Q. Li, X. Qu and D. Zhu, Aggregation Behavior of Dissolved Black Carbon: Implications for Vertical Mass Flux and Fractionation in Aquatic Systems, *Environ. Sci. Technol.*, 2017, **51**, 13723-13732.

5 Y. Yu, A. F. Astner, T. Md. Zahid, I. Chowdhury, D. G. Hayes and M. Flury, Aggregation kinetics and stability of biodegradable nanoplastics in aquatic environments: Effects of UV-weathering and proteins, *Water Res.*, 2023, **239**, 120018.

6 C. J. Van Oss, Hydrophobicity of biosurfaces - Origin, quantitative determination and interaction energies, *Colloids. Surfaces. B.*, 1995, **5**, 91-110.

7 C. J. Van Oss, Long-range and short-range mechanisms of hydrophobic attraction and hydrophilic repulsion in specific and aspecific interactions, *J. Mol. Recogni.* 2003, **16**, 177-190.

8 Y. Xu, Q. Ou, Q. He, Z. Wu, J. Ma and X. Huangfu, Influence of dissolved black carbon on the aggregation and deposition of polystyrene nanoplastics: Comparison with dissolved humic acid, *Water Res.*, 2021, **196**, 117054.

9 B. Vincent, J. Edwards, S. Emmett and A. Jones, Depletion flocculation in dispersions of sterically-stabilized particles (soft spheres), *Colloids Surf.,* 1986, **18**, 61-281.

10 L. A. Wijenayaka, M. R. Ivanov, C. M. Cheatum and A. J. Haes, Improved Parametrization for Extended Derjaguin, Landau, Verwey, and Overbeek Predictions of Functionalized Gold Nanosphere Stability, *J. Phys. Chem. C.*, 2015, **119**, 0064-10075.

11 K. Wang, S. Xu, J. Wang, B. Gao, Y. Huang, J. Song, S. Ma, H. Jia and S. Zhan, Insights into the photosensitivity and photobleaching of dissolved organic matter from microplastics: structure-activity relationship and transformation mechanism, *J. Hazard. Mater.*, 2024, **480**, 135931.

12 C. J. Van Oss, Acid-base interfacial interactions in aqueous media, *Colloids. Surf. A.*, 1993, **78**, 1-49.